PHYSICAL REVIEW A

ATOMIC, MOLECULAR, AND OPTICAL PHYSICS

THIRD SERIES, VOLUME 53, NUMBER 1 JANUARY 1996

ARTICLES

Circular quantum billiard with a singular magnetic flux line

S. M. Reimann,[1] M. Brack,[1] A. G. Magner,[2] J. Blaschke,[1] M. V. N. Murthy[3]

[1]*Institute for Theoretical Physics, University of Regensburg, D-93040 Regensburg, Germany*

[2]*Institute for Nuclear Research, 252028 Prospekt Nauki 47, Kiev-28, Ukraine*

[3]*Institute of Mathematical Sciences, Madras 600 113, India*

(Received 31 July 1995; revised manuscript received 7 September 1995)

We discuss the application of Gutzwiller's semiclassical theory to a circular billiard with a singular magnetic flux line added at its center. The Aharonov-Bohm effect manifests itself through the cancellation of periodic orbits for particular flux strengths. Diffraction phenomena affect the gross-shell structure of the level density and require corrections of higher order in $\hbar$. The full quantization of the level spectrum, however, is much less affected.

PACS number(s): 03.65.Sq, 03.65.Bz, 71.20.Ad, 73.20.Dx

I. INTRODUCTION

Periodic orbit theory (POT) relates oscillations in the quantum level density of a given Hamiltonian to the periodic orbits in the corresponding classical system. The foundations of POT are closely related to the semiclassical quantization introduced by Bohr and Sommerfeld in the early days of quantum mechanics. Classical chaos, however, was the reason for the failure of the semiclassical quantization of the helium atom, and Einstein [1] was the first to point out that the old Bohr-Sommerfeld quantization rules do not apply to classical chaotic motion. The first answer to this puzzle came in 1971, when Gutzwiller presented his famous trace formula, which relates the oscillations in the level density to the periods, actions, and stability angles in the sum over all classical periodic orbits [2–4]. In its simplest form, when all periodic orbits are isolated in phase space, this trace formula reads

$$\delta g(E)=\frac{1}{\pi\hbar}\sum_{\mathrm{PO}}\frac{T_{\mathrm{PPO}}}{\sqrt{|\det(\tilde{M}_{\mathrm{PO}}-I)|}}\cos\left(\frac{S_{\mathrm{PO}}(E)}{\hbar}-\sigma_{\mathrm{PO}}\frac{\pi}{2}\right). \tag{1.1}$$

Each periodic orbit (labeled ''PO'') contributes an oscillating term whose phase is the action integral $S_{\mathrm{PO}}(E)$ along the periodic orbit. The amplitude is a slowly varying function of the energy and depends on the orbit stability and the period T_{PPO} of the primitive periodic orbit (''PPO''); $\tilde{M}_{\mathrm{PO}}$ is the $(2n-2)$-dimensional stability matrix (n is the number of degrees of freedom). The Maslov index σ_{PO} is an integer and depends on the topological features of the dynamics. Formally, the derivation of Eq. (1.1) is based upon a semiclassical approximation to the single-particle propagator, originally proposed by van Vleck in 1928 [5] and rederived by Gutzwiller [2] from Feynman's path integral, and makes use of the method of stationary phases. In the form proposed by Gutzwiller, the trace formula is only applicable if all involved periodic orbits are isolated in phase space. It has therefore been particularly successful in its applications to classically chaotic systems (see Ref. [3] for a review), and finally made the semiclassical quantization of the helium atom possible [6]. The drawback of the method is that it fails for systems which have degenerate families of nonisolated periodic orbits, such as typically occur in integrable systems.

Using a multiple-reflection expansion of the time-independent Green's function and again employing the principle of stationary phases, Balian and Bloch [7] derived in 1972 a trace formula for cavities with ideally reflecting walls of arbitrary shape. Explicit results were given for a spherical cavity in three dimensions, which recently became famous in the context of metal cluster physics [8]. In Refs. [9,10] Gutzwiller's approach was generalized to *integrable* systems, explicitly taking into account the degeneracy of the classical motion in a given potential. A generalization of the Gutzwiller theory to systems which exhibit continuous symmetries has been derived by Creagh and Littlejohn [11].

In the present work, we investigate a two-dimensional circular billiard with a singular magnetic flux line, using the extended Gutzwiller method of Refs. [9,10]. After a short derivation in Sec. II of the semiclassical level density in the circular billiard—which has been discussed before in the literature [12,13]—we show in Sec. III that a singular magnetic

flux line at the center of the disk leads to drastic modifications of the quantum level density. We demonstrate that in the lowest-order POT the effect of the flux line can be described by the addition of the Aharonov-Bohm (AB) phase to the classical action. However, novel diffraction effects arise which modify the gross-shell structure dramatically, although they have only little effect on the fully quantized spectrum. We understand them as AB scattering of a plane wave [14], but their quantitative inclusion in the POT necessitates corrections of higher order in Planck's constant $\hbar$. This is, as yet, an unexplored territory.

The most ambitious use of the semiclassical approach is to identify the individual quantum energies. Summing over sufficiently many periodic orbits in the trace formula, the quantum levels should appear as singularities in the level density. It is well known, however, that the full quantization can only be reached in a few exceptional cases. Very often, one has to deal with severe convergence problems that often can be overcome only by a substantial reordering of the periodic orbit sum or by folding it with a suitable averaging function. Formulating a quantization condition in terms of the dynamical ζ function [15], the semiclassical estimate of quantum energies has also been discussed in Refs. [16]. Using Bogomolny's method [17], the quantization of the circular billiard was addressed in Refs. [18,19]. We show in Sec. IV that a full quantization can be obtained from the trace formula by Gaussian averaging it over a width which is smaller than the spacing of the quantum levels, and summing over a sufficiently large number of periodic orbits. Numerically, this leads to exactly the same eigenvalues as the Einstein-Brillouin-Keller (EBK) quantization [20,21]. This result is far from being trivial, since *a priori* one would expect an agreement of the POT energy levels with EBK only to lowest order in $\hbar$.

II. CLASSICAL PERIODIC ORBITS AND THE LEVEL DENSITY IN THE CIRCULAR BILLIARD

Before investigating the effects of a magnetic flux line on the level density, we first discuss the simple case of the circular billiard with radius R [12,13,19]. In the present work, we show that its level density can as well be derived from Gutzwiller's semiclassical approximation to the Green's function [2,4]. This yields exactly the same trace formula as is obtained by the methods of Balian and Bloch [12] or by Berry and Tabor [13,22,23].

In general, for a quantum system with discrete eigenenergies ε_i the level density $g(E)$ is given by the sum of Dirac δ functions

$$g(E)=\sum_i \delta(E-\varepsilon_i), \tag{2.1}$$

where the sum over i includes the degeneracies. It is common knowledge that the level density $g(E)$ can be split into a smooth and an oscillating part:

$$g(E)=\tilde{g}(E)+\delta g(E). \tag{2.2}$$

For the circular billiard, the *smooth* part $\tilde{g}(E)$ is known analytically [24] to be

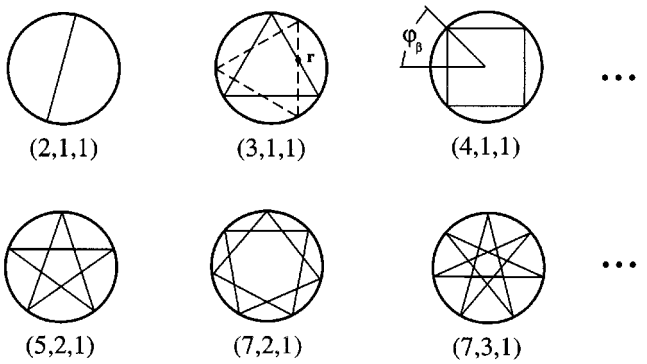

FIG. 1. Periodic orbits in the circular billiard. The straight-line polygons are labeled by the index $\beta=(a,b,n)$, where n is the number of fundamental periods, a is the number of reflections at the boundary during one period, and b measures how many times the path encircles the center per period. For a periodic orbit, the angle $\phi=b\pi/a$ is a rational multiple of π.

$$\tilde{g}(E)=(1-\sqrt{E_0/E})/4E_0, \tag{2.3}$$

corresponding to the the familiar Weyl expansion, with the energy unit $E_0=\hbar^2/2mR^2$. The *oscillating* part $\delta g(E)$ of the level density is the key quantity which the POT relates to the periodic orbits of nonzero length in the corresponding classical system.

The classical dynamics of a circular billiard follows elementary geometry, and due to momentum conservation the motion of the particle is determined only by its direction and position. The periodic orbits for the circular billiard are the regular polygons shown in Fig. 1. Each of these orbits β can be characterized by three integer numbers: $\beta=(a,b,n)$, where n is the number of fundamental periods, a is the number of turning points at the boundary during one period, and b measures how many times the trajectory encircles the center during the fundamental period. Therefore the winding number w around the origin of the disk is given by $w=bn$, and we have the additional condition that $b=1$ for $a=2$ and $b<\frac{1}{2}a$ for $a>2$. The length L_β is then given by

$$L_\beta=2anR\,\sin\varphi_\beta, \tag{2.4}$$

where $\varphi_\beta=b\pi/a$ and R is the radius of the disk.

If the angle φ_β (as displayed in Fig. 1 for the square orbit as an example) is a rational multiple of π, the orbit closes periodically after a reflections. For irrational multiples of π, however, the orbit continuously hits the boundary at different points. With an increasing number of turns around the origin, its trajectory fills a ring-shaped area between its caustic and the boundary. Such an orbit is never repeated, so that it has an infinite period [7,25] and can be omitted from the trace formula.

In Fig. 2 we illustrate for the example $\beta=(3,1,1)$ how any given orbit can be rotated within the boundary without changing its length and thus its classical action. Due to this circular symmetry, we have *degenerate* families of orbits. Therefore Gutzwiller's trace formula (1.1), valid only for isolated orbits, does not apply. However, for the present two-dimensional case, we can still use Gutzwiller's semiclassical Green's function [2–4]

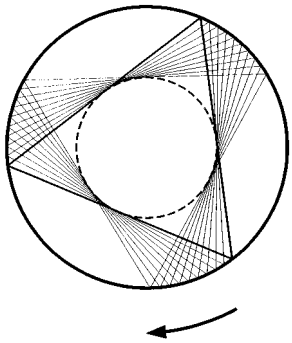

FIG. 2. The family of nonisolated orbits, shown for the triangle $\beta=(3,1,1)$ as an example. Rotation of the periodic orbit within the boundary does not change the value of the classical action.

$$G_{\rm sc}(\mathbf{r}',\mathbf{r}'';E)=2\pi(2\pi\hbar)^{-3/2}\sum_{\text{all paths}}|\mathscr{J}_\beta(\mathbf{p}'t_\beta;\mathbf{r}''E)|^{1/2}\times\exp\left[\frac{i}{\hbar}S_\beta(\mathbf{r}',\mathbf{r}'';E)-i\mu_\beta\frac{\pi}{2}-i\frac{3\pi}{4}\right], \tag{2.5}$$

where the summation goes over *all* classical trajectories β, and take its trace in configuration space to arrive at the level density:

$$\delta g_{sc}(E)=-\frac{1}{\pi}\,\mathrm{Im}\int G_{\rm sc}(\mathbf{r},\mathbf{r};E)\,d^2r. \tag{2.6}$$

In Eq. (2.5), μ_β is the Maslov index [3,26] appropriate for the Green's function, and $\mathscr{J}_\beta(\mathbf{p}'t_\beta;\mathbf{r}''E)$ is the Jacobi determinant for the transformation between the variables $(\mathbf{p}'t_\beta)$ and $(\mathbf{r}''E)$. $S_\beta(\mathbf{r}',\mathbf{r}'';E)=\oint\mathbf{p}\cdot d\mathbf{q}$ is the classical action integral along the path from $\mathbf{r}'$ to $\mathbf{r}''$. By taking the trace in Eq. (2.6), the integration over the area covered by the orbits, i.e. the ring area between the circular boundary and their caustic, takes account of the degeneracy of the orbits. For any given point $\mathbf{r}$ between the caustic ($r=R_c=R\cos\varphi_\beta$) and the boundary ($r=R$), there exists a periodic orbit crossing this point. Therefore, we have a continuum of periodic orbits $\beta=\beta(a,b,n)$ of a given family filling the ring area between the caustic and the boundary, all of which have the same values of the classical action. Hence, the action S_β corresponding to the family of orbits β is constant and does not depend on the choice of the point $\mathbf{r}$, and can therefore be taken outside the trace integral.

Note that in the standard derivation of Gutzwiller's trace formula (1.1), the stationary phase approximation is used for the integrations in the directions perpendicular to the orbits, which leads to the condition of periodicity. In the present case, the actions and thus the phases are identically constant in the above mentioned ring areas. The stationary phase approximation can therefore not be used as it would lead to diverging integrals. Instead, the trace integrals over these areas can be done exactly, as discussed below. Still, it appears as a reasonable approximation to restrict the sum in Eq. (2.5) to *periodic* orbits, since the contributions from nonperiodic closed orbits will essentially be canceled by rapid phase oscillations, when the point $\mathbf{r}$ at which such an orbit intersects itself is varied in the radial direction.

For the circular billiard we arrive at the following trace formula:

$$\delta g_{\rm sc}(E)=-\frac{2}{(2\pi\hbar)_{3/2}}\,\mathrm{Im}\sum_\beta f_\beta\exp\left[\frac{i}{\hbar}S_\beta-i\sigma_\beta\frac{\pi}{2}-i\frac{3\pi}{4}\right]\times\int d\mathbf{r}|\mathscr{J}_\beta(\mathbf{p}'t;\mathbf{r}''E)|^{1/2}, \tag{2.7}$$

where the sum now runs over the set of distinct families $\beta(a,b,n)$ of periodic orbits for a given energy E. The factor f_β is the number of different orbits of a given family passing through the point $\mathbf{r}$. For $a=2$ (diameter orbit) we have $f_\beta=1$ and for $a>2$ (all polygons) we have $f_\beta=2$. This difference in the amplitudes for the diameter and the closed polygons comes from the fact that for $a>2$, at any point $\mathbf{r}$ we have two different orbits which are symmetric with respect to the axis (0, $\mathbf{r}$) (see Fig. 1). The integral in Eq. (2.7) is done exactly over the ring area between the circular boundary and the caustic of each orbit family and can, in fact, be performed analytically.

In Ref. [10] it has been shown that, using the Hamilton-Jacobi equations and a local coordinate system (x,y) in which x is directed along the orbit and y is perpendicular to it, the Jacobian $\mathscr{J}_\beta$ simplifies to

$$\mathscr{J}_\beta=\left(\frac{m}{p}\right)^2\left(\frac{\partial p_y'}{\partial y''}\right)_\beta. \tag{2.8}$$

The derivative $(\partial p_y'/\partial y'')_\beta$ determines the displacement of the final point $\mathbf{r}$ in the direction of the y axis due to the variation of the initial momentum projection p_y'. This is a characteristic of the stability of the corresponding orbit. Introducing the angle θ_p' by $p_y'=p\sin\theta_p'$, we have for $\theta_p'\ll1$

$$\mathscr{J}_\beta=\frac{m^2}{p}\left(\frac{\partial\theta_p'}{\partial y''}\right)_\beta. \tag{2.9}$$

For cylindrical symmetry, the Jacobian $(\partial\theta_p'/\partial y'')_\beta$ equals [9,10]

$$\left(\frac{\partial\theta_p'}{\partial y''}\right)_\beta=\frac{R\sin\varphi}{2an(r^2-R^2\cos^2\varphi)}. \tag{2.10}$$

It now remains to determine the Maslov index σ_β in Eq. (2.7). For each periodic orbit β, this phase is determined by the number of conjugate points along the path β [3,26]. Any simple conjugate point changes the value of σ_β by one unit and thus gives a phase shift of $-\pi/2$ in the level density. For all orbits, we have at each reflection from the boundary a simple turning point related to the sign change of the normal component of the particle momentum and a caustic point in the tangential direction to the boundary, leading to $\Delta\sigma=2$ per reflection (which gives an overall phase change of $-\pi$ as in classical wave optics). In the interior of the billiard, there are conjugate points along the caustic (shown by the dashed

line in Fig. 2) of each orbit. We finally obtain the following analytical trace formula for the oscillating part of the level density:

$$\delta g_{\rm sc}(E)=\frac{1}{E_0}\frac{1}{\sqrt{\pi kR}}\sum_{\beta=(a,b,n)} f_\beta \frac{\sin^{3/2}\varphi_\beta}{\sqrt{an}}\sin\Phi_\beta, \tag{2.11}$$

where

$$\Phi_\beta=kL_\beta-3an\frac{\pi}{2}+\frac{3\pi}{4}. \tag{2.12}$$

Here E is the energy of the particle, $k=\sqrt{2mE}/\hbar$ the wave number, and f_β has been defined after Eq. (2.7). In the overall phase Φ_β, the term kL_β is the classical action S_β of the orbit β in units of $\hbar$. Recently, Eq. (2.11) has also been derived by Tatievski *et al.* [12], applying an extension of the Balian-Bloch theory for cavities with a finite depth, and by Creagh [13], using the method of Ref. [11].

To avoid convergence problems of the sum in Eq. (2.11), we average the level density over a finite energy interval. This is similar in spirit to Balian and Bloch [7], who gave the energy a small imaginary part. The coarse graining of semiclassical and quantum-mechanical level densities is by now a standard practice, and the ability of the trace formula to reproduce the coarse-grained level density fairly accurately has been demonstrated for a large number of systems (see, e.g., Refs. [10,12,16]). Here we convolute the semiclassical level density over the variable k with a Gaussian of width γ/R, which gives for each orbit β an extra damping factor $\exp(-\gamma^2L_\beta^2/4R^2)$ in all terms of the periodic orbit sum Eq. (2.11). This is equivalent to averaging the quantum level density E with a width $2\gamma\sqrt{EE_0}$.

For the circular billiard, the exact eigenenergies ε_i are given, in units of E_0, by the squared zeros of the cylindrical Bessel functions with integer indices $\Lambda=0,\pm1,\pm2,\ldots$. We choose an averaging range $\gamma=0.6$ which corresponds to a coarse graining of the level density that preserves its gross-shell structure. The lowest part of Fig. 3 shows both the averaged quantum-mechanical and the semiclassical $\delta g(E)$: their difference can hardly be recognized.

So far, our present investigation is nothing more than a reduction of the well-known three-dimensional spherical billiard [7] to two dimensions, and altogether the results described above are not surprising. In the next section, however, we want to examine the influence of a pure gauge field on the motion of the particle in quantum mechanics, and study the effect of length scales in the quantum-size regime. We will demonstrate that the presence of a vector potential yields characteristic differences between the classical and quantal behavior, and discuss how these changes may be included in the semiclassical level density.

III. CIRCULAR AHARONOV-BOHM BILLIARD

In the following, we discuss the changes in the classical and quantum dynamics of the charged point particle, when a magnetic flux line is added at the origin of the disk and perpendicular to the x-y-plane. The level statistics of the so-called Aharonov-Bohm billiards have been investigated

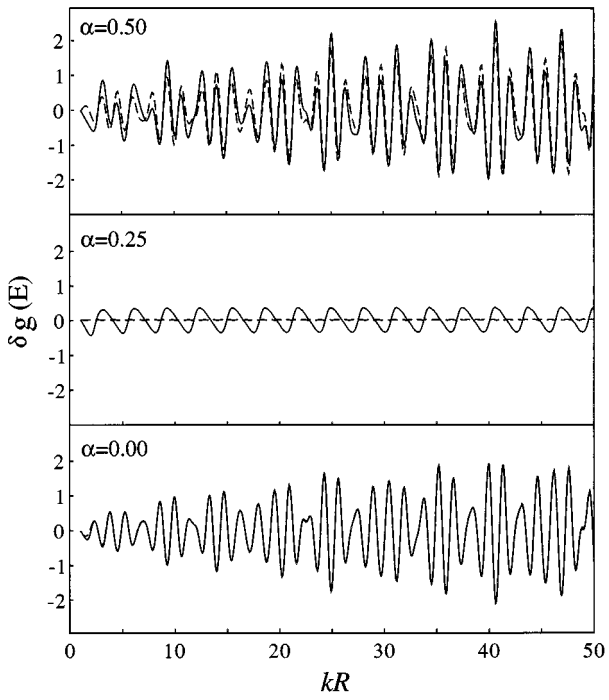

FIG. 3. Oscillating part of the level density in the Aharonov-Bohm disk billiard with magnetic flux strength $\alpha=0$ (bottom), 0.25 (middle), and 0.5 (top). We have plotted $\delta g(E)$ versus kR, Gaussian convoluted with $\gamma=0.6$ and multiplied by the norm factor $2\gamma(\pi EE_0)^{1/2}$. Dashed lines, coarse-grained quantum results; solid lines, semiclassical results Eq. (3.7), correspondingly averaged.

by Berry and Robnik [27] for cases where the geometry of the boundary causes chaotic dynamics, and by Date *et al.* [28] for rectangular boundaries, where the system is pseudo-integrable.

Again restricting the calculations to two dimensions, the Lagrangian is given by

$$\mathscr{L}=\frac{1}{2}m\mathbf{v}^2+\frac{e}{c}\mathbf{v}\cdot\mathbf{A}, \tag{3.1}$$

where $\mathbf{A}$ denotes the vector potential, which in a symmetric gauge is given by [29]

$$\mathbf{A}(\mathbf{r})=\frac{\phi}{2\pi}\left(\frac{-y}{x^2+y^2}\mathbf{e}_x+\frac{x}{x^2+y^2}\mathbf{e}_y\right), \tag{3.2}$$

and $\phi/2\pi$ is the flux through the solenoid. This corresponds to a magnetic field $\mathbf{B}$ which has a δ function singularity at the origin and is zero everywhere else:

$$\mathbf{B}=\nabla\times\mathbf{A}=\phi\delta^{(2)}(\mathbf{r})\mathbf{e}_z. \tag{3.3}$$

With Eq. (3.2), the Lagrangian Eq. (3.1) in cylindrical coordinates (r,θ) simplifies to

$$\mathscr{L}=\frac{1}{2}m(\dot r^2+r^2\dot\theta^2)+\frac{e\phi}{2\pi c}\dot\theta. \tag{3.4}$$

As a consequence of the well-known Aharonov-Bohm effect [14], the wave function of the particle acquires a flux-dependent phase change upon rotation around the solenoid.

For a nonzero flux ϕ, the particle is classically not allowed to penetrate the flux line, because its energy would become infinite. For $r \neq 0$, the Lorentz force on the particle is always zero and the classical equations of motion remain unchanged. This can easily be seen from Eq. (3.4), because the interaction term due to the flux line in the Lagrangian is a total time derivative. The geometries of the classical orbits with $a > 2$ in the configuration space therefore do not change. The quantum spectrum, however, does depend on the flux ϕ.

For integer values of the canonical angular momentum Λ, the energy eigenvalues and wave functions are determined by solving the corresponding radial part of the Schrödinger equation, with the dimensionless flux strength $\alpha = e\phi/hc$,

$$\frac{\hbar^2}{2m}\left(-\frac{1}{r}\frac{\partial}{\partial r}r\frac{\partial}{\partial r}+\frac{1}{r^2}(\Lambda-\alpha)^2\right)\Psi_i=\varepsilon_i\Psi_i\,, \qquad (3.5)$$

with Dirichlet boundary conditions $\Psi_i(R)=0$. The quantity $(\Lambda-\alpha)^2$ can take fractional values, if we assume that α can take a continuous range of values between 0 and 1. The boundary condition together with the condition of normalisability of the quantal wave functions finally yield the energy eigenvalues as

$$\varepsilon_i=\varepsilon_{|\Lambda-\alpha|,n}=E_0X^2_{|\Lambda-\alpha|,n}\,,$$

$$\text{where} \quad J_{|\Lambda-\alpha|}(X_{|\Lambda-\alpha|,n})=0. \qquad (3.6)$$

We see that the presence of the flux line in the circular billiard simply changes the order of the Bessel functions from integer to fractional [27]; the symmetry $\alpha \leftrightarrow (1-\alpha)$ in the quantum spectrum allows the restriction to $0 \leqslant \alpha \leqslant 0.5$. For *integer* flux $\alpha = 0,1,2,\ldots$, the quantum spectrum is unaltered by the flux line. This is easily seen from the fact that for any integer value of α the angular momentum gets redefined and the new set is isomorphic to the old one both in terms of the spectrum and eigenstates. This mapping, however, has no classical analog since the classically allowed angular momenta remain the same.

In the numerical computation, all zeros $X_{|\Lambda-\alpha|,n} \leqslant 100$ of $J_{|\Lambda-\alpha|}(x)$ are included. Figure 3 shows the oscillating level density $\delta g(E)$ (solid lines) for $\alpha=0.25$ (middle) and for $\alpha=0.5$ (top), averaged and plotted in the same way as for $\alpha=0$ at the bottom. Clearly, the gross-shell behavior undergoes dramatic changes when the flux strength α is varied.

In order to understand this behavior of the level density, let us now inspect the Fourier spectra of $\delta g(\sqrt{E})$ of the AB disk which give us directly the lengths of the involved classical periodic orbits. The coarse graining with $\gamma=0.6$ suppresses all but the shortest orbits. In Fig. 4 we show the (absolute) Fourier amplitudes for different values of α. For $\alpha=0$ (bottom) we have the spectrum of the simple disk billiard; the visible signals correspond to the orbits with $n=1$ (lowest harmonics) for $a=2$ (diameter), 3 (triangle), 4 (square), 5 (pentagon). For increasing α the height of these peaks is reduced, until at $\alpha=0.25$ virtually no trace is left of the classical orbits with length $L \geqslant 4R$. For $\alpha > 0.25$ they

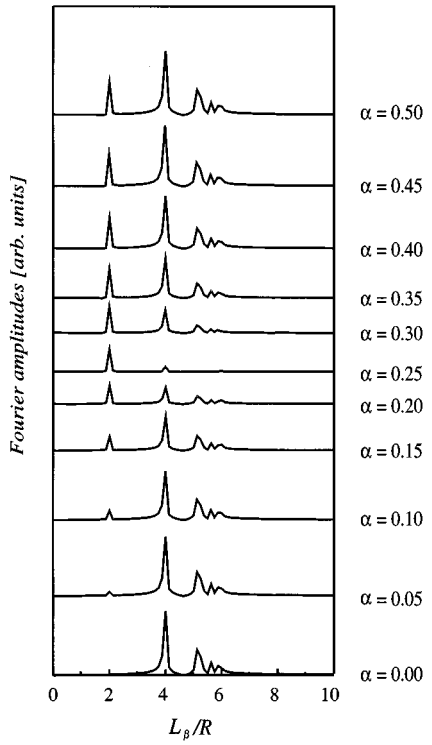

FIG. 4. Fourier spectra of the quantum level density $\delta g(E)$, with $\gamma=0.4$ and normalization as in Fig. 3, for the Aharonov-Bohm circular billiard with various flux strengths α. Note how for $\alpha=0.25$ all signals, except those of the half-diameter orbit and its harmonics, disappear due to the Aharonov-Bohm effect.

appear again. Their disappearance at $\alpha=0.25$ is a simple consequence of the Aharonov-Bohm effect, as we shall see below.

Two other features are particularly noteworthy in Fig. 4. First, the peak at $L=4R$ exists also for $\alpha > 0$, although the classical diameter orbit is forbidden, and undergoes the same cancellation at $\alpha=0.25$. Second, there appears a new signal at $L=2R$, corresponding to a ''reflected'' half-diameter orbit, with an amplitude that increases with α up to $\alpha=0.5$. Both phenomena can be interpreted quantum mechanically. When a wave hits the flux line, it is diffracted; part of it is reflected and part is transmitted. Thus the two signals at $L=2R$ and $L=4R$ correspond to the reflected and the transmitted wave, respectively. The fact that the $L=4R$ peak is suppressed at $\alpha=0.25$ is obviously due to the possibility of the wave to bypass the flux line on either side: the two events pick up opposite phases, so that their contributions cancel exactly at $\alpha=0.25$ as in the classical Aharonov-Bohm experiment. (For $\alpha=0.25$, the tiny signals at $L=4R$ and, hardly visible, at $L=6R$ and $8R$ are actually the higher harmonics with $n=2,3,4$ of the reflected half-diameter orbit.)

The squared Fourier peak at $L=2R$ in Fig. 4 as a function of α can be fitted by $\sin^2(\pi\alpha)$ within the numerical accuracy, as shown in Fig. 5. This is precisely the AB cross section for backward scattering: indeed, the quantum-mechanical cross section for scattering of a plane wave by a singular magnetic flux is proportional to $\sin^2(\pi\alpha)/\cos^2(\theta/2)$, where θ is the scattering angle [14]. This strongly supports our interpretation of the $L=2R$ peak for $\alpha \neq 0$ as a simulated classical half-diametric orbit resulting

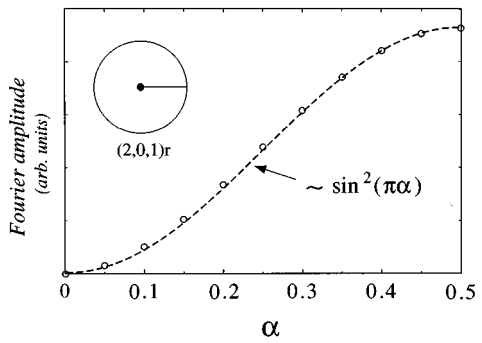

FIG. 5. Quantum Fourier amplitudes of the reflected orbit of length $L_\beta=2R$ in the Aharonov-Bohm disk as a function of flux strength α.

from a reflection by the flux line. The quantitative amplitudes describing these diffraction phenomena in POT will appear as quantum corrections of higher order in $\hbar^{1/2}$.

Let us now interpret these results in terms of POT. As a consequence of the well-known Aharonov-Bohm effect [14], the wave function of a particle acquires a phase $2\pi\alpha$ upon each rotation around the flux line. Classically, the anyonic gauge term does not affect the equations of motion. However, the canonical angular momentum p_θ is changed to $p_\theta+\alpha\hbar$, so that the classical action S_β acquires as an extra contribution the AB phase which here amounts to $\pm 2\pi\alpha bn$, the sign depending on the orientation of the orbit [27,28]. To lowest order, we therefore expect that the orbits with $a>2$, whose geometry is not affected by the flux line, give the contribution

$$\begin{aligned}\delta g_{\rm sc}(E,\alpha)&=\frac{1}{E_0}\frac{1}{\sqrt{\pi kR}}\sum_\beta f_\beta\frac{\sin^{3/2}\varphi_\beta}{\sqrt{an}}\\&\quad\times 1/2\,[\sin(\Phi_\beta+2\pi\alpha bn)\\&\quad+\sin(\Phi_\beta-2\pi\alpha bn)]\\&=\frac{1}{E_0}\frac{1}{\sqrt{\pi kR}}\sum_\beta f_\beta\frac{\sin^{3/2}\varphi_\beta}{\sqrt{an}}\\&\quad\times\sin(\Phi_\beta)\cos(2\pi\alpha bn).\end{aligned}\tag{3.7}$$

This corresponds to a ''minimal inclusion'' of the AB effect into the trace formula. In Ref. [31] a similar investigation was made for the nonintegrable Hénon-Heiles potential, in which the classical motion is chaotic at higher energies. The treatment of the diametric orbits ($a=2$) is less clear: classically, they are forbidden since the linear canonical momenta diverge at the origin [28], and the particle cannot penetrate the flux line; wave mechanically, we expect diffraction. From the behavior of the Fourier peaks at $L=4R$, however, we conclude that the diametric orbit ($a=2$), which represents the transmitted wave, should also be added by the ''minimal AB inclusion'' to the sum in Eq. (3.7).

Equation (3.7) now simply explains the disappearance of all peaks in the Fourier spectrum which correspond to orbits with winding number $nb=1$: the two sine functions including the opposite AB phases cancel exactly at $\alpha=0.25$. From Eq. (3.7) it follows that the Aharonov-Bohm effect cancels all periodic orbits with a winding number $bn=(2i+1)/4\alpha$ with integer $i=0,1,2\ldots$.

It is interesting to note that, starting from a minimal inclusion of the Aharonov-Bohm phase in the semiclassical EBK spectrum, Eq. (3.7) can be obtained using the Poisson summation formula and then performing the integrations by the stationary phase method (see, e.g., [23]). For a cylinder, such investigations have already been carried out by Bogachek and Gogadze [30], who obtained from the EBK spectrum a trace formula for a cylindrical confinement, which is identical to the result of the Balian-Bloch theory given in Ref. [12]. The results of Ref. [30] anticipate the more general theory of semiclassical quantization in integrable systems given later by Berry and Tabor [22].

Note that our findings are substantiated by the isotropic two-dimensional harmonic oscillator with singular magnetic flux line, for which the quantum-mechanical trace formula is known analytically [31].

Diffraction effects similar to those discussed above can also be found in a disk billiard with a concentric inner reflecting boundary with radius R_i in situations where R_i is comparable to or smaller than the de Broglie wavelength of the particle. (The semiclassical trace formula for this system has been derived by Tatievski *et al.* [12]; the nonconcentric case has been studied by Bohigas *et al.* [32].) The semiclassical diffraction from circular hard-wall scatterers with finite size has been investigated recently by Wirzba [33] and Vattay *et al.* [34], taking into account diffracted rays in addition to the geometrical ones. Scattering resonances between two confocal hyperbolae were studied by Whelan [35], and in Refs. [36,37] a discussion of the n-disk scatterer can be found, showing that POT approximates the energies and widths of the scattering resonances to great accuracy. Pavloff and Schmit investigated diffraction effects in two-dimensional polygonal billiards and give an analytical trace formula accounting for the diffractive orbits [38]. Finally, $\hbar$ corrections to the Gutzwiller trace formula by means of an asymptotic power series have been discussed by Gaspard and Alonso [39] for hyperbolic systems.

IV. FULL QUANTIZATION AND EBK THEORY

So far, we have only discussed the application of POT to the coarse-grained level density, which works equally well in both nonintegrable and integrable systems, where a full quantization can only be reached in a few exceptional cases [3]. It is well known, however, that integrable systems can be quantized using the EBK method [20]. We therefore now attempt a full quantization of the disk billiard, starting from Eq. (2.11). We choose a very small averaging range $\gamma=0.02$ which corresponds to an energy interval much smaller than the shortest interval occurring between the lowest 14 quantum levels. At the bottom of Fig. 6 we show the semiclassical result for $\alpha=0$. Indeed, we obtain an almost perfect quantization (the maximum length of orbits included here was $L_m=30\,000R$). The peaks are displaced with respect to the exact levels (shown by small circles along the energy axis) by about 2% for the lowest eigenvalue, and by fractions of a percent around $kR\approx 15$. The exact degeneracies (1 for $\Lambda=0$ and 2 for $\Lambda\neq 0$) are obtained with a signal-

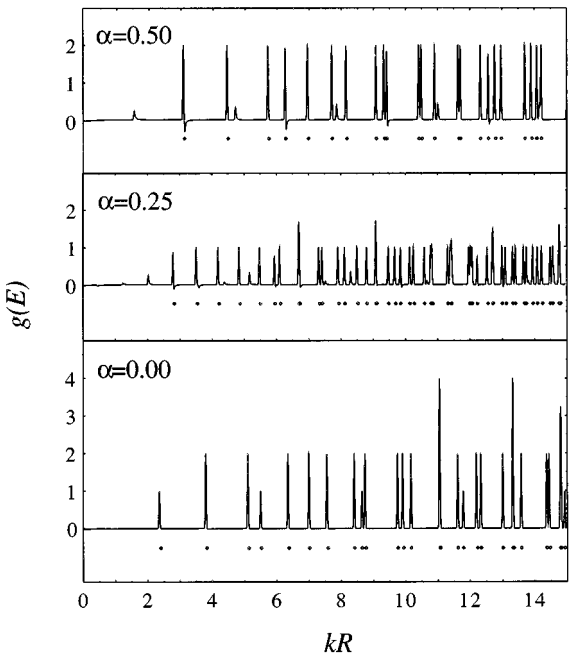

FIG. 6. Semiclassical total level density $g_{sc}(E,\alpha)$, as sum of $\tilde{g}(E)$ in Eq. (2.3) and δg_{sc} in Eq. (3.7), for the Aharonov-Bohm disk billiard, normalized and plotted as in Fig. 3, for three values of the magnetic flux strength α. The averaging width was $\gamma=0.02$; orbits with maximum length 30 000R were included in the sum of Eq. (3.7). The small circles indicate the positions of the exact quantum-mechanical eigenvalues.

to-noise ratio better than 1000:1. (The three higher spikes correspond to accidental near degeneracies which cannot be resolved with $\gamma=0.02$.) We get the same result [21] also for the three-dimensional spherical billiard [7,9,10]: the level positions are of the same quality as obtained in the EBK method, and the exact degeneracies $2\Lambda+1$ are obtained for the states with orbital angular momentum Λ [21].

Berry and Tabor [22] have developed a semiclassical theory which starts from EBK quantization and applies to systems with degenerate orbits. They derived a trace formula that is similar to the sum over periodic orbits obtained by Gutzwiller and concluded that both methods, where they apply, should lead to equivalent results. This can be expected to be true *to lowest order in* $\hbar$, but not necessarily beyond since in both approaches, some higher-order terms in $\hbar$ are omitted automatically when the saddle-point approximation is used to derive the trace formula. The equality of the two approaches was confirmed by a recent alternative generalization of Gutzwiller's theory for systems with continuous symmetries by Creagh and Littlejohn [11]; for integrable systems without higher dynamical symmetries, such as the circular disk billiard, the trace formula of Berry and Tabor has, indeed, been rederived in Ref. [11]. Moreover, the trace formula for the circular billiard, as well as for a cylindrical billiard in three dimensions, can be obtained by Poisson summation of the EBK energies, using again the method of stationary phases, and the resulting formulas are identical [23,30].

All this strongly suggests that the EBK quantization and Gutzwiller's approach not only agree to lowest order in $\hbar$ but give, in fact, *identical* spectra. We have confirmed this numerically by our calculations, which show that the relative difference between the EBK and POT eigenvalues is smaller than 10^{-8}, whereas the relative difference between EBK and the exact quantum energies is of the order of 10^{-1} to 10^{-2}. The details of these numerical calculations are given in the Appendix.

For the disk billiard including the magnetic flux line, the EBK spectrum is modified, like the exact one, by subtracting the flux strength α from the angular momentum Λ. Using the "minimal AB inclusion" Eq. (3.7) for $\delta g_{sc}(E,\alpha)$, which ignores all possible higher-order corrections in $\hbar$, we get the results shown in Fig. 6 for $\alpha=0.25$ (middle) and $\alpha=0.5$ (top). The exact degeneracy for $\alpha=0.25$ is 1 for all levels (except for accidental degeneracies), for $\alpha=0.5$ it is 2. The heights of most peaks correspond to these degeneracies, and their positions are of the same accuracy as for $\alpha=0$. Some small structures of alternating sign can be seen for $\alpha\neq 0$ which do not correspond to eigenvalues; their height is much smaller than unity and decreases with smaller averaging widths. For $\alpha=0.5$, the period of these small peaks with one given sign is π; in the chosen units this corresponds to the period of the reflected half-diametric orbit whose contribution to the trace formula we have ignored. It is expected that the correct inclusion of the quantum corrections stemming from the diffraction effects will remove these structures. But even without these corrections, we obtain from Eq. (3.7) a fairly good spectrum of comparable quality to that for $\alpha=0$.

Our above discussion on possible differences between EBK and POT eigenvalues may be further clarified by the following observation. If one starts from the EBK spectrum of the AB disk and performs a Fourier transform of the corresponding level density, one finds results very similar to those shown in Fig. 4 which contain a clear signal from the reflected diameter orbit. Thus the EBK level density does contain a corresponding $\hbar$ correction term. By Poisson resummation of the EBK level density and *applying the saddle-point approximation*, one obtains [23,30] exactly our POT result quoted in Eq. (3.7), showing that all $\hbar$ correction terms are lost in the process of the saddle point approximation. The simple disk billiard ($\alpha=0$) must be considered as a particularly fortunate case where no further errors (beyond those inherent in the EBK approximation) are introduced in the derivation of the trace formula. (Similar fortunate cases are the harmonic oscillator potentials, for which the POT spectra even coincide analytically with the exact quantum-mechanical spectra [40].)

V. SUMMARY AND CONCLUSIONS

In summary, we have shown that the inclusion of a singular magnetic flux line in a circular billiard leads to significant modifications of the coarse-grained quantum level density. The most dramatic changes can be interpreted as due to the Aharonov-Bohm effect and are incorporated into the lowest-order POT simply by adding the AB phase to the action appearing in the trace formula, leading to Eq. (3.7). The diffraction effects caused by the flux line also modify the gross-shell structure appreciably, but are less important for the full quantization of the spectrum. The Fourier com-

ponent corresponding to a particle reflected by the flux line has an amplitude proportional to the AB backward scattering amplitude, as was also found analytically for a two-dimensional harmonic oscillator potential with magnetic flux line. The quantitative treatment of the diffraction effects within the POT necessitates the inclusion of higher-order corrections in $\hbar$. Summing over sufficiently long orbits, we numerically obtain from Eq. (3.7) a full quantization that is identical to the EBK result, at least for the disk without flux line. We can therefore conclude that the extended Gutzwiller theory, that of Balian and Bloch [7], and that of Berry and Tabor [22] for the integrable case of the disk billiard are all equivalent in giving exactly the spectrum obtained by the EBK quantization.

ACKNOWLEDGMENTS

It is a pleasure to thank R. K. Bhaduri, S. Creagh, and N. Whelan for discussions and many helpful comments. Two of us (A.G.M. and M.V.N.M.) acknowledge the financial support by the Universitätsstiftung Hans Vielberth which made their visits at Regensburg University possible. This work has been supported by the Commission of the European Communities, Grant No. SG1*CT920770, and by INTAS, Grant No. 93-0151.

APPENDIX: NUMERICAL EVLUATION OF THE POT EIGENVALUES

This appendix deals with the numerical determination of the ''POT eigenvalues'' (e.g., the peak positions of the POT level density in the limit of a vanishing smoothing width γ) in the case of the circular billiard without flux line. The results show with high accuracy that the POT eigenvalues are identical to those of the EBK quantization. The difference between the two semiclassical methods is at least six orders of magnitude smaller than the semiclassical error, e.g., the difference to the exact quantum-mechanical result. This is non-trivial, as we expect the semiclassical approximations to agree only up to the order of the semiclassical error.

1. Determining the POT eigenvalues

Even in integrable systems, the PO sum is in general not absolutely converging. The sum is therefore not well defined, as it depends on the summation order. Standard practice to overcome these convergence problems is a so-called ''smoothing'' of the PO sum [16]. The method consists of folding the PO sum with a ''smoothing function'' of width γ. We use an equivalent approach which exploits the close analogy of the PO sum to discrete Fourier transformation [41]. We multiply the amplitudes of the PO sum with an appropriate window function $W(L)$, which is nonzero only on $[-L_m, L_m]$. Here L denotes the orbit length, hence L_m is the maximum orbit length taken into account. The equivalent smoothing width γ is proportional to $1/L_m$. This approach enables us to compensate most of the errors due to the unavoidable truncation of the infinite PO sum in our calculation, which improves the accuracy remarkably. We are interested in the peak positions P of the POT level density in the limit of vanishing smoothing, e.g., for $L_m \to \infty$. We therefore calculate the positions $P(L_m)$ for various L_m. If it is possible to fit a simple function to $P(L_m)$, one can extrapolate $P(L_m)$ for $L_m \to \infty$. In contrast to the method of taking the position for a sufficiently large L_m as an approximation to the position for $L_m = \infty$, this strategy gives control over the convergence behavior. Furthermore, the accuracy is again improved, as machine precision sets bounds on the maximum L_m that can practically be handled.

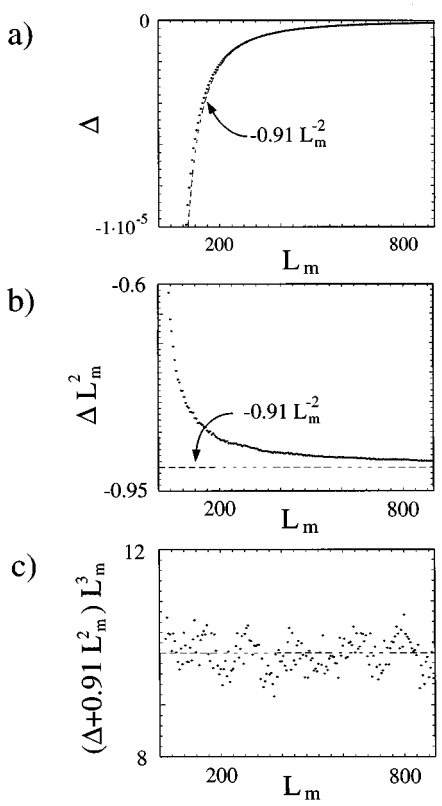

FIG. 7. (a) Difference Δ between the EBK eigenvalue $\varepsilon^{\mathrm{EBK}}$ and $P(L_m)$. The dotted line is proportional to L_m^{-2}. (b) The quantity ΔL_m^2 seems to converge to a constant, showing the first term in $P(L_m)$ to be of the order L_m^{-2}. (c) The L_m^2 term is compensated; plotting the remainder multiplied by L_m^3 against L_m shows that the next term is of the order L_m^{-3} (dotted line). The spreading of the data points is proportional to L_m^{-3}, as is expected.

2. POT eigenvalues of the circular billiard

Since we have no theoretical prediction for the dependence $P(L_m)$, we have to guess it by inspection. The data of Fig. 7 were calculated with a triangular window for the eigenvalue with $\Lambda=1$, $n=1$. Figure 7(a) shows the difference Δ between the EBK value and $P(L_m)$. The dotted line is proportional to L_m^{-2}. The diagram strongly suggests that the leading term of Δ is of the order L_m^{-2}. This is confirmed in Fig. 7(b), showing that ΔL_m^2 converges to a constant. In Fig. 7(c) the L_m^2 term is compensated; plotting the remainder multiplied by L_m^3 against L_m shows that the next term is of the order L_m^{-3}. Higher-order terms in $P(L_m)$ cannot be observed. The spreading of the data is proportional to L_m^{-3}, as is expected for the triangular window [41]. These observations suggest fitting $P(L_m)$ by the function

TABLE I. Differences between some POT and EBK eigenvalues compared with the difference between EBK and the exact quantum result.

	$\Lambda=0$, $n=1$	$\Lambda=0$, $n=2$	$\Lambda=1$, $n=1$	$\Lambda=2$, $n=1$
$\lvert\text{EBK}-\text{POT}\rvert$	1.8×10^{-9}	2.1×10^{-9}	3.2×10^{-9}	3.9×10^{-9}
$\lvert\text{EBK}-\text{QM}\rvert$	4.9×10^{-2}	2.2×10^{-2}	3.7×10^{-2}	3.5×10^{-2}

$$\tilde{P}(L_m)=\varepsilon_i^{\text{EBK}}+c_1+\frac{c_2}{L_m^2}+\frac{c_3}{L_m^3}, \tag{A1}$$

with three parameters c_i. All other investigated eigenvalues behave in the same way; using another window function changes mainly the behavior of the spreading of the data.

We calculated four POT eigenvalues, using a triangular window and a window function which is a triangle folded with a rectangle. Extrapolating $L_m\to\infty$ gives c_1 as an estimate for the difference between the POT and the EBK eigenvalues. This value is, within the numerical accuracy, independent of the chosen window function, as would be expected. The parameters that control the convergence behavior, c_2 and c_3, do depend on the window function. The results are listed in Table I.

3. Comparing POT, EBK, and quantum-mechanical eigenvalues

The EBK eigenvalues are given [20] by the roots $E=\varepsilon_i^{\text{EBK}}$ of the equation

$$\begin{aligned}&|\Lambda|\arcsin(2|\Lambda|\sqrt{E_0/E})+2\sqrt{E/E_0-\Lambda^2}\\&\quad=\pi(2n+|\Lambda|-1/2).\end{aligned} \tag{A2}$$

The quantum-mechanical eigenvalues are given by the zeros of the Bessel functions, as described in Sec. II. Both EBK and quantum-mechanical eigenvalues were calculated to an accuracy of 0.5×10^{-16}. In Table I we compare the differences between some POT and EBK eigenvalues with the difference between EBK and the exact quantum result.

The EBK and the quantum-mechanical results are not identical. This is not surprising, since EBK is only an approximation up to first order in $\hbar$. As POT is another approximation of the quantum-mechanical level density to first order, we would expect the EBK and POT eigenvalues to agree up to this accuracy only. But the typical error of the semiclassical approximation is at least seven orders of magnitude larger than the difference between POT and EBK, which is smaller than the numerical accuracy for the POT eigenvalues. This strongly suggests that the two semiclassical methods give exactly the same eigenvalues.

[1] A. Einstein, Verh. Dtsch. Phys. Ges. **19**, 82 (1917).
[2] M. C. Gutzwiller, J. Math. Phys. **10**, 1004 (1967); **11**, 1791 (1970); **12**, 343 (1971).
[3] M. C. Gutzwiller, *Chaos in Classical and Quantum Mechanics* (Springer-Verlag, New York, 1990).
[4] M. C. Gutzwiller, in *Chaos and Quantum Physics*, Les Houches Session L11, edited by M. J. Giannoni, A. Voros, and J. Zinn-Justin (Elsevier Science Publishers, B. V., New York, 1991).
[5] J. H. van Vleck, Proc. Natl. Acad. Sci. USA **14**, 178 (1928).
[6] D. Wintgen, K. Richter, and G. Tanner, Chaos **2**, 19 (1992).
[7] R. Balian and C. Bloch, Ann. Phys. (N.Y.) **69**, 76 (1972).
[8] M. Brack, Rev. Mod. Phys. **65**, 677 (1993).
[9] V. M. Strutinsky, Nukleonika **20**, 679 (1975).
[10] V. M. Strutinsky and A. G. Magner, Fiz. Elem. Chastis At. Yadra **7**, 356 (1976) [Sov. J. Part. Nucl. **7**, 138 (1976)].
[11] S. C. Creagh and R. G. Littlejohn, Phys. Rev. A **44**, 836 (1991); J. Phys. **A 25**, 1643 (1992).
[12] B. Tatievski, Diploma thesis, Freie Universität Berlin, 1993; B. Tatievski, P. Stampfli, and K. H. Bennemann, Comput. Mater. Sci. **2**, 459 (1994).
[13] S. Creagh, Ann. Phys. (N.Y.) (to be published).
[14] Y. Aharonov and D. Bohm, Phys. Rev. **115**, 485 (1959).
[15] M. V. Berry and J. P. Keating, J. Phys. A **23**, 4839 (1990).
[16] M. Sieber, Chaos **2**, 35 (1992); M. Sieber and F. Steiner, Phys. Rev. Lett. **67**, 1941 (1991); C. Matthies and F. Steiner, Phys. Rev. A **44**, R7877 (1991).
[17] E. B. Bogomolny, Nonlinearity **5**, 805 (1992).
[18] T. Szeredi, J. Lefebvre, and D. Goodings, Nonlinearity **7**, 1463 (1994).
[19] P. A. Boasman, Nonlinearity **7**, 485 (1994).
[20] J. B. Keller, Ann. Phys. (N.Y.) **4**, 180 (1958); J. B. Keller and S. I. Rubinow, Ann. Phys. (N.Y.) **9**, 24 (1960).
[21] M. Brack, S. C. Creagh, P. Meier, S. M. Reimann, and M. Seidl, in *Contribution to NATO Advanced Study Institute "Large Clusters of Atoms and Molecules"*, Erice, 1995, edited by T. P. Martin (Kluwer, Dordrecht, in press).
[22] M. V. Berry and M. Tabor, Proc. R. Soc. London, Ser. A **349**, 101 (1976); J. Phys. A **3**, 371 (1977).
[23] F. von Oppen, Ph.D. thesis, University of Washington, 1993.
[24] H. P. Baltes and E. R. Hilf: *Spectra of Finite Systems* (Bibliographisches Institut, Zürich, 1976), p. 59.
[25] M. V. Berry, Eur. J. Phys. **2**, 91 (1981).
[26] M. V. Fedoryuk, *Asymptotics: Integrals and Sums* (Nauka, Moscow, 1987) (in Russian).
[27] M. V. Berry and M. Robnik, J. Phys. A **19**, 649 (1986).
[28] G. Date, S. R. Jain, and M. V. N. Murthy, Phys. Rev. E **51**, 198 (1995).
[29] A. Lerda, *Anyons*, Lecture Notes in Physics, Monographs Vol. m4 (Springer, Berlin, 1992).
[30] E. N. Bogachek and G. A. Gogadze, Zh. Éksp. Teor. Fiz. **63**, 1839 (1972) [Sov. Phys. JETP **36**, 973 (1973)].
[31] M. Brack, R. K. Bhaduri, J. Law, C. Meier, and M. V. N. Murthy, Chaos **5**, 317 (1995), Eq. (22) (δ there is the α of the

present paper). The first line in this equation corresponds exactly to the ''minimal AB inclusion,'' applied to *all* orbits (including the pendular orbit crossing the flux line); the remaining terms are explicit $\hbar$ corrections. Note also the appearance of the factor $\sin(\pi k\delta)$ in the last term which corresponds to an orbit reflected by the flux line.

[32] O. Bohigas, D. Boosé, R. Egydio de Carvalho, and V. Marvulle, Nucl. Phys. **A560**, 197 (1993).

[33] A. Wirzba, Chaos **2**, 77 (1992).

[34] G. Vattay, A. Wirzba, and P. E. Rosenqvist, Phys. Rev. Lett. **73**, 17 (1994).

[35] N. Whelan (unpublished).

[36] B. Eckhardt, J. Phys. A **20**, 5971 (1987).

[37] P. Cvitanovic and B. Eckhardt, Phys. Rev. Lett. **63**, 823 (1989).

[38] N. Pavloff and C. Schmit (unpublished).

[39] P. Gaspard and D. Alonso, Phys. Rev. A **47**, R3468 (1993).

[40] M. Brack and S. R. Jain, Phys. Rev. A **51**, 3462 (1995).

[41] We plan to published a detailed discussion of the nature of the analogy between PO sums and Fourier transforms in the future.